ISSN 0742-0463, Journal of Volcanology and Seismology, 2024, Vol. 18, No. 1, pp. 64–77. © Pleiades Publishing, Ltd., 2024.

Neotectonics of the Barents Sea Shelf Eastern Part: Seismicity, Faults and Impact of the Atlantic–Arctic Rift System

S. Yu. Sokolov[a], *, A. S. Abramova[a], S. I. Shkarubo[b], R. A. Ananiev[c], E. A. Moroz[a], and Yu. A. Zaraiskaya[a]

[a] *Geological Institute, Russian Academy of Sciences, Pyzhevsky per., 7, str. 1, Moscow, 119017 Russia*

[b] *Marine Arctic Geological Expedition Co., ul. Sofii Perovskoi, 26, Murmansk, 183038 Russia*

[c] *Shirshov Institute of Oceanology, Russian Academy of Sciences, Nakhimovsky prosp., 36, Moscow, 117218 Russia*

**e-mail: sysokolov@yandex.ru*

Received April 15, 2023; revised October 12, 2023; accepted October 20, 2023

Abstract—This study analyzes seismicity within the shelf of the Barents Sea and the Knipovich and Gakkel ridges that surround it, and compares the spatial distribution of seismicity with the fault network as identified by seismic prospecting data. Kinematic characteristics have been obtained for the spatial migration of seismic activity. It is shown that the seismic events recorded by NORSAR, the Norwegian regional network, as occurring within the Russian part of the Barents Sea shelf make linear clusters along strike slip faults. The fault network displaces Mesozoic seismic sequences and emerges at the bottom surface by displacing Quaternary deposits. This clearly indicates a present-day age of the faults along which the linear clusters of low magnitude seismicity aligned. The computation of the total seismic moment in the space-time domain showed the presence of a seismic activity migration along short fault segments in the shelf at rates of 10.5 to 25.7 km/year. A burst of general activity in the shelf area beginning in 2012 could be noted. Comparison of the time-dependent evolution of seismic activity in the shelf to fragments of the Atlantic–Arctic Rift System suggests that the evolution is due to tectonic deformation waves that are initiated along the geodynamically active plate boundary and are propagating to the shelf at a rate of 20–22 km/year. Another alternative, namely, that the rate of migration can reach 77 km/year, is less likely. The increase in the rate of seismic activity in the shelf after 2012 might be, not emission due to the excitation of a slow deformation wave, but rather resulted from direct triggering impact on the shelf by the Knipovich and Gakkel ridges.

Keywords: seismicity, Knipovich and Gakkel ridges, neotectonics, Barents Sea, seismic sections, fault network, migration rate of seismic activity

DOI: 10.1134/S0742046323700409

INTRODUCTION

The subject of our research in neotectonics within the eastern part of the Barents Sea shelf is related to the presence of a geodynamically active frame of the sea and the continent–ocean transition zone (Fig. 1). There are two nearly perpendicular segments of the Atlantic–Arctic Rift System (AARS) to the northwest near passive continental margins and shelves in Eurasia, namely, the Knipovich Ridge (with the Lena Trough) and the Gakkel Ridge. According to (*USGS ...,* 2022), the ridges are characterized by intensive seismicity that is typical for tensional mid-oceanic ridges. Quaternary volcanoes have been identified in the Spitsbergen Archipelago (Sirotkin and Sharin, 2000) along with lateral movements at lithosphere top as seen from GPS data (Heflin et al., 2020; *GPS ...,* 2022) occurring at a rate of 17.9 mm/year at azimuth 36° (see Fig. 1). There is another evidence for active geodynamics within the shelf, namely, the presence of an anomalously hot mantle beneath the Spitsbergen Archipelago and environs (Gac et al., 2016), which is not typical for continental shelf areas in the Arctic region (Yakovlev et al., 2012). This is confirmed by riftogenic values of heat flow as measured in the Orly Trough during the 25th cruise of the R/V *Akademik Nikolai Strakhov*; the heat flow is 550 mW/m^2, which is by ~8 greater than the background values for shelves (Khutorskoi et al., 2009). According to regional seismic tomography studies (Bungum et al., 2005), the northwestern angular part of the Barents Sea shelf has beneath it a depression in the isosurface of P-wave 8.3 km/s value (Sokolov et al., 2023a), which too indicates an uncommon rheologic state of the mantle beneath the continental region.

The eastern part of the shelf has a feature of its own, namely, a fault network (Harrison et al., 2008) which was confidently identified based on data of structural seismic prospecting and is completely displayed in the state geological maps to scale 1 : 1 000 000 for the eastern Barents Sea (*Karta ...,* 2004). The network con-

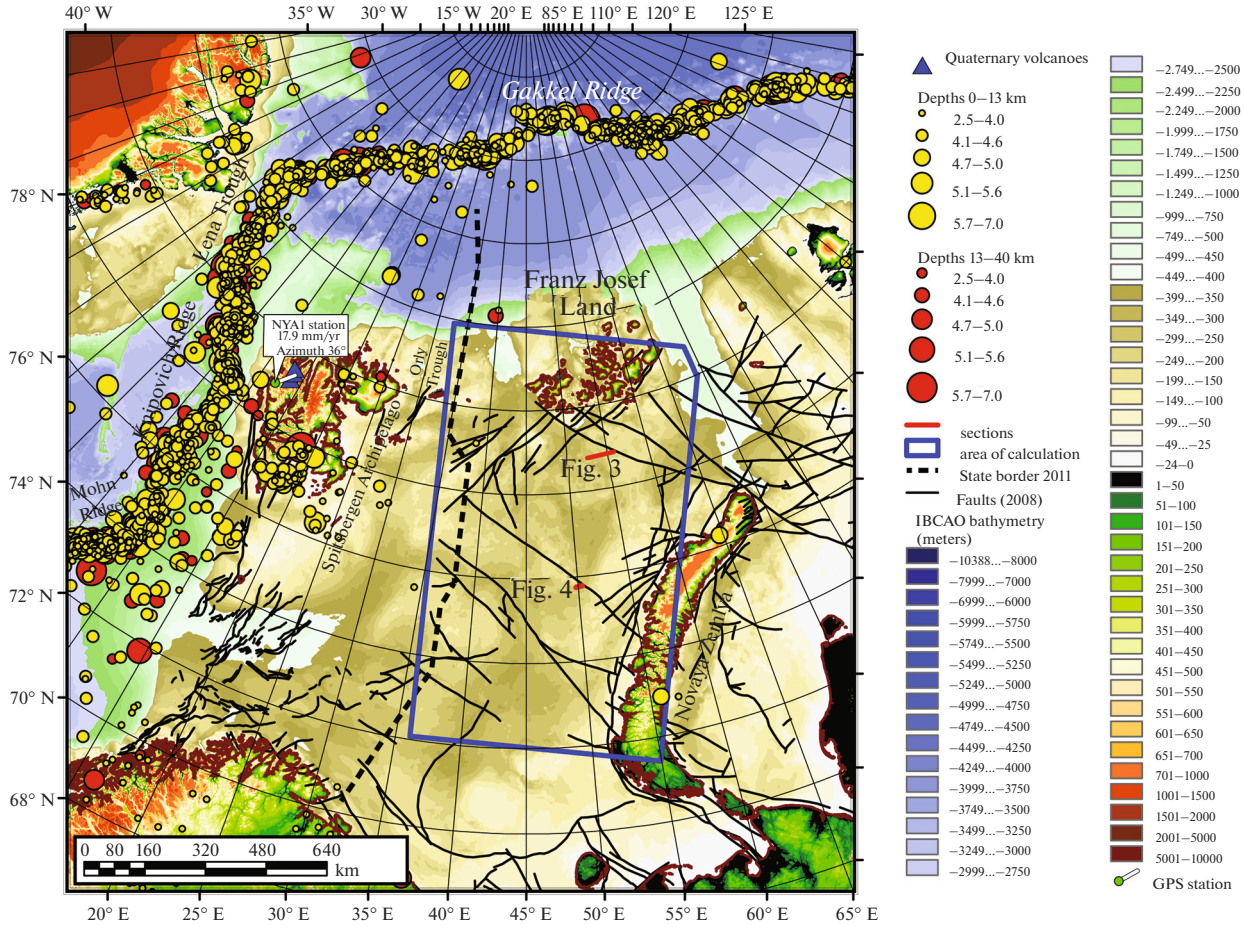

Fig. 1. The seismicity of the northwestern framing of the Barents Sea shelf based on data from (*USGS* ..., 2022) for events with magnitudes greater than 2.5, separately for the depth ranges 0–13 and 13–40 km; the fault network is after (Harrison et al., 2008), the Quaternary volcanoes were borrowed from (Sirotkin and Sharin, 2000), and the parameters of motion for the GPS NYA1 station are based on data from (Heflin et al., 2020; *GPS* ..., 2022). Also shown are the area of calculation for the space–time evolution of total moment release due to low magnitude seismic events as reported in (*NORSAR* ..., 2022) for the period 2001–2020 (the dark blue triangle) and segments of sections (red lines). The topographic base is from IBCAO data (Jakobsson et al., 2020).

tains left lateral faults striking at an angle of ~45° with respect to the continental margin (see Fig. 1). The faults are not shown in the Norwegian part of the sea owing to insufficient information incorporated in the international geological map (Harrison et al., 2008). Comparison of the strike slip faults with deep mantle cross sections in the tomographic model (Bungum et al., 2005) carried out by Sokolov et al. (2023a) demonstrates a relationship between their geometry and mantle inhomogeneities. An analysis of fault data given in more detail (Nikitin et al., 2018) revealed that the faults are accompanied by a "dense" feather network which is not shown in maps to scale 1 : 1000000. Studies of the upper sedimentary section for the Barents Sea and of its seismicity (Musatov, 1998; Krapivner, 2007; Antonovskaya et al., 2021) showed that the sea area contains numerous elements of neotectonics and seismic activity occurring far beyond the divergent plate boundaries (see Fig. 1), and is subject to the impact of tectonic deformation waves. These facts together with the data (Sokolov et al., 2023b) on the eastward spatial migration of the junction zone between the Knipovich and Mohn ridges indicate a geodynamic impact of active structures on the shelf and its possible tectonic activation developing eastward and northeastward. The present paper is devoted to an analysis of interrelationships shown by shelf faults, teleseismic data, and regional seismicity based on the data of (*NORSAR* ..., 2022).

REGIONAL SEISMICITY AND FAULTS

The Barents Sea seismicity as inferred from data of the regional network (*NORSAR* ..., 2022) (Fig. 2) indicates the existence of intraplate events with epicenters clustering parallel to the shelf break with strike slip source mechanisms; the slip planes are oriented nearly north–south (Olesen et al., 2000) and there is a nearly east–west tension (Keiding et al., 2018). These data indicate tectonic activation of the shelf close to its

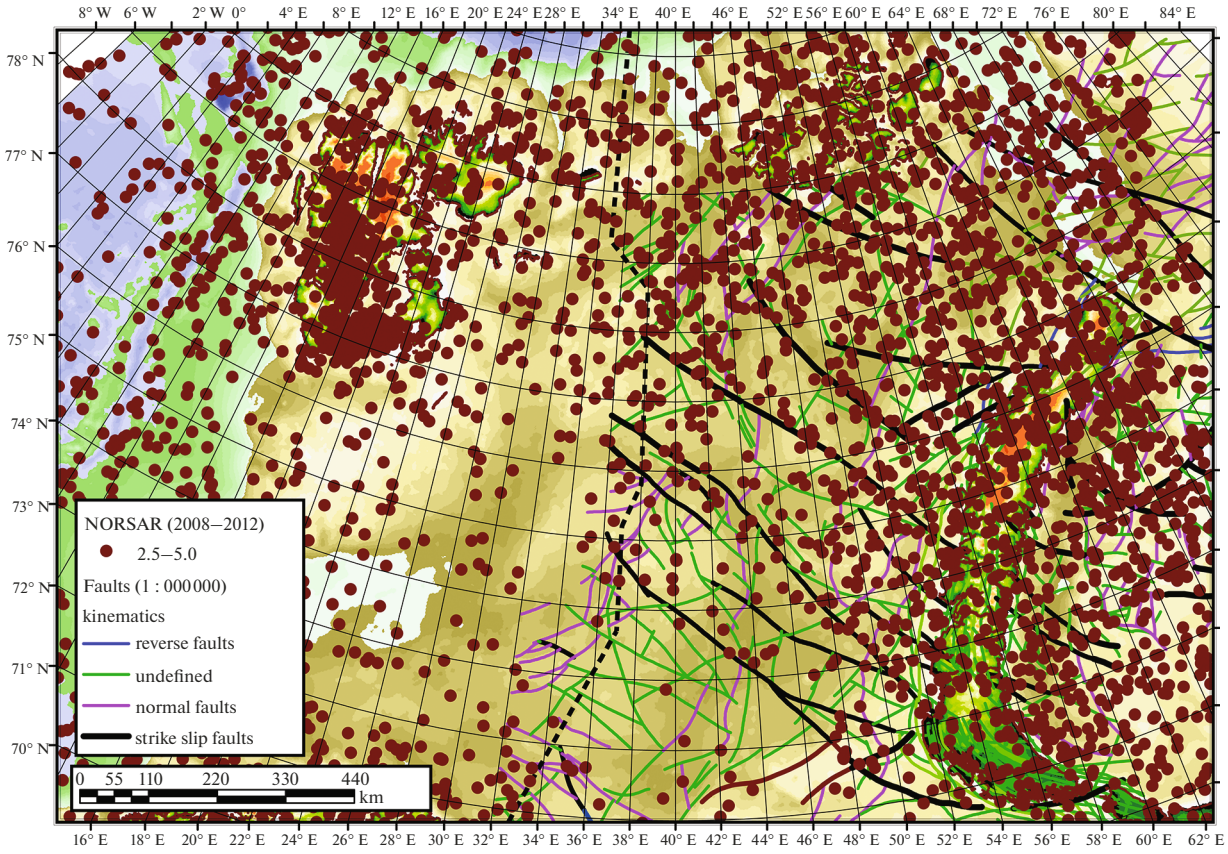

Fig. 2. Seismicity of the Barents Sea shelf based on data of (*NORSAR* ..., 2022) for the period 2008 to 2012 for events with magnitudes greater than 2.5. The fault network is based on GIS data of the State Geological Map of the Russian Federation, scale 1 : 1 000 000 (the New Series) with faults indication by kinematic type (*Karta* ..., 2004).

western margin, and a possible eastward migration (Sokolov et al., 2023b). Data visualization (*NORSAR* ..., 2022) for magnitudes greater than 2.5 for the period of observation between 2008 and 2012 shows that the epicenters in the northeastern Barents Sea are grouped into linear chains striking northwest (see Fig. 2). This is the only location in the eastern part of the sea where NORSAR data (*NORSAR* ..., 2022), which largely come from detection of random noise spikes, showed clustering of these events to make linear clusters (see Fig. 2), which are radically different from a chaotic distribution. Comparison of their spatial distribution to the fault network inferred for the project of the State Geological Map of the Russian Federation to scale 1 : 1 000 000 (the New Series) (*Karta ...,* 2004) shows that the events are confined to left lateral strike-slip faults and the accompanying feather faulting, which can well fail to be shown in a map of this scale. The well-pronounced western cluster is not merely located along a fault, but also experiences the same bend in strike near the area with coordinates ~44° E and ~77° N. In the case under consideration, a large statistics upon the background of detections with a chaotic spatial distribution reveals the same weak events, but which exhibit a clear spatial correlation; this is absent from events generated by a really random process; the correlation is also found to be confined to a present-day tectonic feature. We note that the rate of events associated with faults increases as one approaches the Novaya Zemlya fold–thrust structure and decreases to the south of the sea area. We believe that the association between clusters and faults is not sporadic, and it is fault structures which host the tremor source.

The northern continent–ocean transition zone in the Barents Sea manifests itself in seismicity as recorded by the Arkhangelsk seismological network (Morozov et al., 2014, 2015). These data are represented by events that align themselves along the shelf break, which A.N. Morozov and coauthors interpreted as resulting from the isostatic response to the load at the continent–ocean boundary. In addition, Morozov et al. (2014, 2015) identified events related to crustal destruction in the area of the northern troughs, which are associated with heat flow showing riftogenic values (Khutorskoi et al., 2009). The process is related to the presence of an anomalously hot mantle in the northwestern framing of the Barents Sea shelf (Bungum et al., 2005), which is also invoked to explain the Quaternary volcanism in the Spitsbergen Archipelago (Sirotkin and Sharin, 2000) and the high seis-

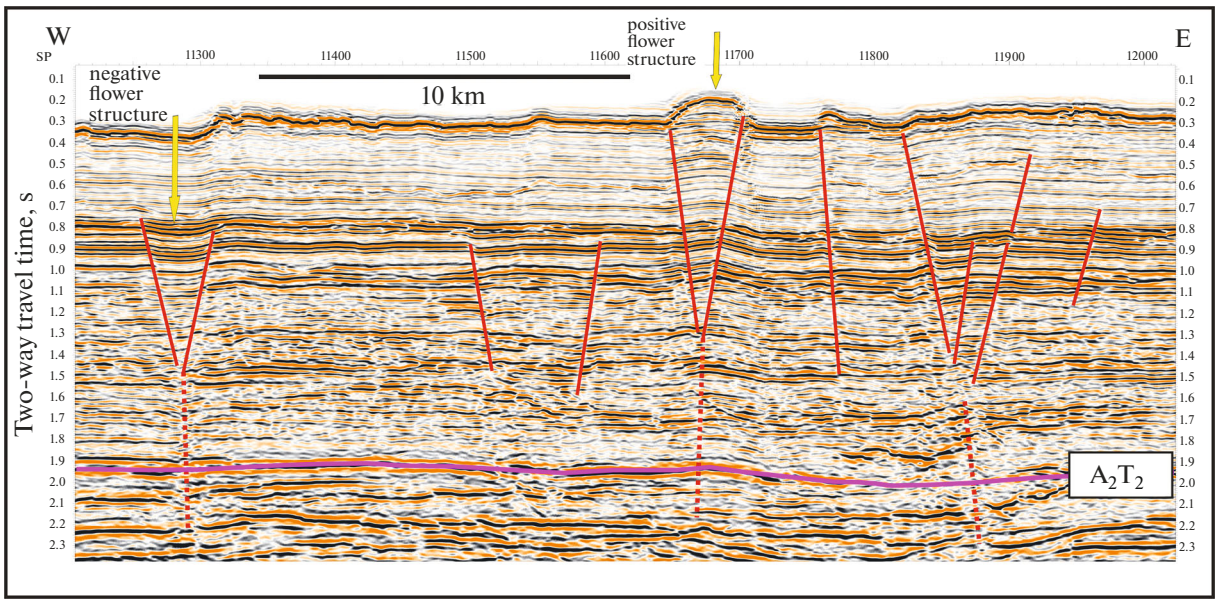

Fig. 3. A fragment of the reference seismic section 4-AR in the northern Barents Sea crossing the northwestern zone of strike slip faults (see Figs. 1 and 2). Solid red lines represent reliably identified faults and the feathering of negative and positive flower structures emerging at the bottom surface. Dashed red lines mark main strike slip faults. The violet line shows the reference Triassic horizon $A_2(T_2)$. The location of the fragment is displayed in Fig. 1.

micity at its southern framing (*ISC* ..., 2023), which is analyzed in the present study.

The project of geological mapping at scale 1 : 1000000 involved a considerable amount of data supplied by structural 2D seismic prospecting the sections of which show absolutely reliable faults. Figure 3 shows a segment of the section where one can see a set of faults emerging at the bottom surface. This short segment contains positive and negative flower structures indicating the existence of a complex mosaic consisting of transtension and transpression regimes near the strike slip fault zone. Similar discontinuities have been identified near strike slip faults further south in the northeastern Barents Sea (Sokolov et al., 2023a). The faults can be traced as far as the sea bottom, hence very likely indicate a present-day age of these discontinuities and their ongoing activity producing a relief-forming effect (see Fig. 3). The detailed study of the uppermost sediment section (USS) (Fig. 4) carried out during the 51st cruise of the R/V *Akademik Boris Petrov* clearly shows faults emerging at the bottom surface as identified from combinations of relief roughnesses and displacements of a high-amplitude bottom reflector, and which show differently directed kinematics. If the resolution of seismic data and the effective length of the bottom reflection are ~40–50 ms (see Fig. 3), then the effective length on a seismogram with dislocations as shown in seismoacoustic sections (see Fig. 4) quite fits this interval. This demonstrates the character of emergence for deep-seated faults onto the surface in high frequency sections without masking by intensive bottom reflections as recorded by deep 2D seismic prospecting.

The USS of the sedimentary rock sequence in different parts over the Barents Sea (Solheim et al., 1998) is characterized by strong variability in composition, thickness of unconsolidated Quaternary deposits, and diamicton (Krapivner, 2018; Dunaev et al., 1995). These overbed eroded Mesozoic complexes (Shipilov and Shkarubo, 2010) displacements of which along the deep-seated fault network are transmitted to the USS. Frozen rocks (Krapivner, 2018) and BSR (a bottom simulated reflector, which is a pseudo-bottom reflector at the bottom of gas hydrates) is a trap for fluids in the form of free gas, and enhance the dynamics of bottom reflectors near deep-seated faults emerging at the surface along which degassing is occurring. Accumulations of gas enhance the amplitude contrast of displaced reflectors and the reliability of fault identification. The data tremor is obviously confined (*NORSAR* ..., 2022) to these fault structures (see Fig. 2), but the interpretation of its origin is not so obvious.

THE DATASET

The illustration of the AARS seismicity is based on data from the catalog at (*USGS* ..., 2022) obtained for the region of study using an oceanic velocity model showing the location of the epicenter cloud without displacement away from the axis of the rift system (see Fig. 1). Calculations of characteristics of the seismic process for the western Barents Sea were based on data from the catalog (*ISC* ..., 2023). The events of the

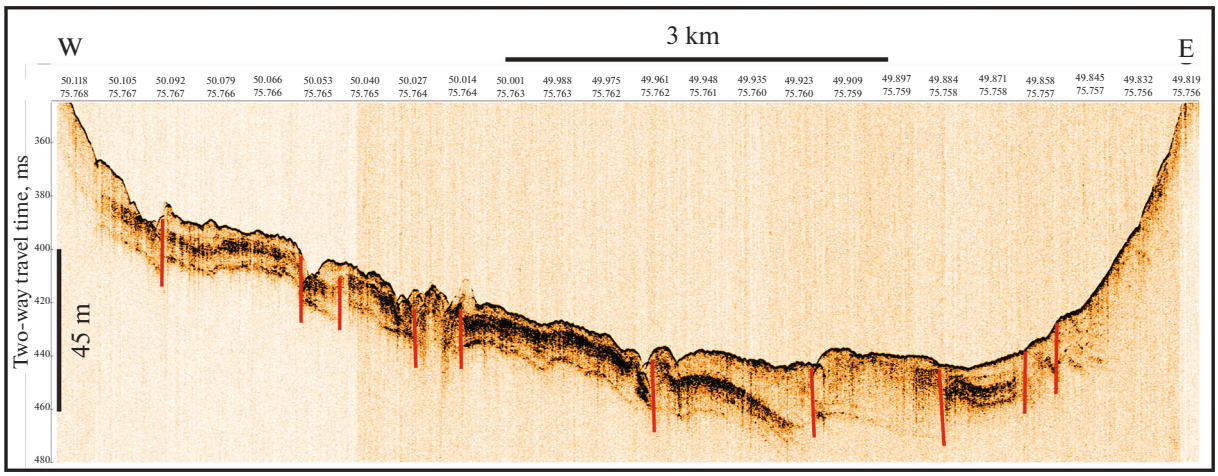

Fig. 4. A fragment of the seismoacoustic section ABP51_2209212244 obtained by a ParaSound P-35 high frequency profiler during the 51st cruise of the R/V *Akademik Boris Petrov* (October–November 2022, Institute of Oceanology RAS, Geological Institute RAS) in the middle of the Barents Sea. The section crosses the northwestern zone of strike slip faults. Red lines show normal and reverse faults that disturb the section top and emerge at the sea bottom. The location of the fragment is shown in Fig. 1.

regional catalog (*NORSAR* ..., 2022) (see Fig. 2) were obtained by automatic detection of time and coordinates using the detailed velocity model NORSAR3D (Ritzmann et al., 2007), which is characteristic for the continental structure of shelves and incorporates the delamination of the crust into the sedimentary and the crystalline layers. The interval 2008–2012 for Fig. 2 was selected with a purpose, since an event with M_w = 6.1 occurred in the southern Spitsbergen on February 21, 2008, which triggered a considerable microseismic response within the archipelago. This activity within the shelf is unique; the geodynamic aspects of its occurrence in the area are discussed in (Sokolov et al., 2023a, 2023b). The regional NORSAR network records events with magnitudes upwards from –2 within the entire area of the Barents Sea by automatic detection, which mostly produces false detections. The occurrence of a spatial correlation (see Fig. 2) shows that the array of automatically detected chaotic events contains a fraction of equally weak events, but which are geometrically confined to faults with neotectonic activity, events that can be interpreted as resulting from the processes going on along these crustal discontinuities. As well, as will be shown later on, these faults exhibit a tendency of space–time displacement that is totally absent from the bulk of the study area. Linear clusters of events are identified over time, as well as over spatial coordinates. This rules out the possibility of a random configuration for the (*NORSAR* ..., 2022) seismicity for the part of the sea area studied here.

For our study we selected events between 2001 and 2020, with the total number of events recorded by two or more stations being ~550 thousands. This amount of automatically detected events makes the results of their linear spatial location statistically significant, in spite of the presence of wrong detections. The emergence of deep-seated faults at the bottom surface is illustrated using materials from the Russian Geological Foundation. The illustration of faults in the USS relied on data which were acquired using a ParaSound P-35 high frequency profiler during the 51st cruise of the R/V *Akademik Boris Petrov* (October–November 2022, Institute of Oceanology and Geological Institute, Russian Academy of Sciences).

COMPUTATIONAL TECHNIQUES

Available data on seismic events (a total of about 550 thousand) for 20 years can be used to produce a statistically significant picture of their spatial distribution in the Barents Sea area, including its Russian part. We calculated the total seismic moment both for the AARS axial part (separately for the Knipovich and Gakkel ridges) based on USGS data and for the events occurring within the shelf area based on NORSAR data using the well-known empirical moment–magnitude Gutenberg–Richter formula. For these calculations we used the coefficients after (Boldyrev, 1998) who studied the seismic process in the North Atlantic. We calculated total released moment for each year starting in 1950 for the AARS segments as indicated. The calculation for the shelf area was carried out for that which was mostly in the Russian part as shown in Fig. 1. The totals were calculated for spatial 10 × 10-km squares at intervals of one year from 2001 to 2020. The result was to obtain a three-dimensional data array (cube), which allowed us to represent the total moment in 3D form with possible options of making 2D vertical slices in its orthogonal sections. The vertical slices of the cube are shown in Fig. 5. The NORSAR catalog, which contains ~240 thousand events with magnitudes upward of –2 in the calculation region (see Fig. 1) was processed using a FORTRAN-90 pro-

gram module compiled specially to deal with the problem. We summed moments of all events to make a 3D array where the X and Y axes are coordinates in the UTM37 projection with the option of adjusting the discretization step, while the Z axis is the third dimension with a time discretization step of one year. The results of these calculations were uploaded into the software module to do a 3D data visualization, as well as to get an integrated sample along one of the axes and to average it in a moving window.

THE RESULTS

The space–time trends of the seismic moment can be traced only in some parts of the cube, namely, in the northern part of the area near northwest-trending strike slip faults and in the eastern part where the strike slip faults join the Novaya Zemlya structures (see Fig. 2). Figure 5 shows an east–west and a north–south section across the total moment cube where we can easily discern trends of this space–time migration of moment maxima at a rate of ~10.5 km/year away from the Knipovich Ridge eastward (see Fig. 5a) and at a rate of ~12.0 km/year from the Gakkel Ridge southward within the Novaya Zemlya area (see Fig. 5b). The remaining space of the cube mostly shows a chaotic distribution of individual total moment peaks. We note the increase in seismic moment compared with the background values since 2015. The increase is best expressed near the northwestern framing of Novaya Zemlya where the archipelago is in contact with the system of strike slip faults (see Fig. 2).

As to the sea area, the best-pronounced linear cluster of events (see Fig. 2) is that alongside the longest strike slip fault in the northeastern Barents Sea; further north it becomes a set of faults of undefined type of kinematics and with an azimuth change of 10° –15° northward. We highlight, in Fig. 6, the area of that cluster for which we made a special selection from the total data array for the period from 2001 to 2020. The space-time distribution of events in the area is shown in Fig. 7. One notes two zones of seismic activity moving southeastward at rates of ~22.8 and ~25.7 km/year. The components of these rate vectors when projected onto the X axis would have the values similar to those highlighted in the orthogonal east–west section in Fig. 5a. There is a silent interval in seismicity near the southern zone lasting ~4 years within which activity decays. A synchronous burst of activity is seen in 2012 within the entire fault zone, with the burst coinciding with the event of June 22, 2012 whose magnitude is 4.18 (see Fig. 6). Since 2016, the synchronous activity along the entire fault zone became more frequent. As is shown in Fig. 6, several events of magnitude greater than 3.8 were recorded in 2016, 2018, and 2020 which are related to the occurrence of synchronous activity (see Fig. 7).

DISCUSSION OF THE RESULTS

The trends derived by our analysis, namely, the movement of seismic activity east of the Knipovich Ridge and south of the Gakkel Ridge (see Figs. 5a, 5b) nicely fit the hypothesis of a superposition of tectonic deformation waves due to two geodynamically active AARS segments framing the northwestern Arctic shelf (Antonovskaya et al., 2021). At the same time, the geometry of the active AARS segments at the two ridges is such as to make these two segments join almost at an angle of 90° (see Fig. 1). Assuming that the ridge push is one of the three main driving forces for the plate tectonic mechanism (Khain and Lomidze, 2005), we must conclude that this situation must have produced a special pattern of the structural tectonic compression elements in the shelf quadrant confined within the two AARS segments, striking at angles of ~45° with respect to both of the ridges (Fig. 8). Actually however, we see no such deformations proceeding from the AARS segments at identical directions. The geodynamic setting in the Knipovich Ridge area is transtension (tension combined with shear) (Verba et al., 2000; Crane et al., 2001; Gusev and Shkarubo, 2001; Zykov and Baluev, 2008; Kutinov et al., 2015; Sokolov et al., 2017; Zaraiskaya, 2017; Sokolov et al., 2023b), indicating different forces that are due to the Gakkel and Knipovich ridges and which act on the Barents Sea shelf. We have the fact that the spreading at the Knipovich Ridge has an oblique direction with respect to the tension axis and its flanks involve deformation occurrences of shear origin. Therefore, the simplified pattern of the force directions that are commonly assumed for active rift structures is inapplicable in this case. The geodynamics of the region acquires a more realistic interpretation involving a right lateral component in the displacement of the plate east of the Knipovich Ridge (see Fig. 8). This easily explains the left strike-slip kinematics of northwest striking faults in the eastern Barents Sea. The system of left lateral strike-slip displacements (see Figs. 1, 2, 8) oriented northwestward at an angle of ~45° with respect to both ridges is quite reliably identified throughout the Barents Sea, and the seismicity is associated with it (see Fig. 2). According to (Shipilov, 2004, 2015; Vinogradov et al., 2005), the Devonian–Triassic rift system and its Jurassic–Cretaceous activity have a system of transform faults whose spatial orientation is identical with that of the faults identified to exist in the maps (*Karta* ..., 2004). This indicates an inheritance relationship of areas of present-day neotectonics to Paleozoic and Mesozoic structural inhomogeneities, but also raises the issue of the geodynamic mechanism that is driving the block-structured plate. The trends as identified here can be due both to movements on faults owing to asymmetrical pressure on the part of the AARS segments or to emission as the deformation waves pass through a fault inhomogeneity. It would be more likely to hypothesize a combination of the two factors. It seems impossible at present to separate

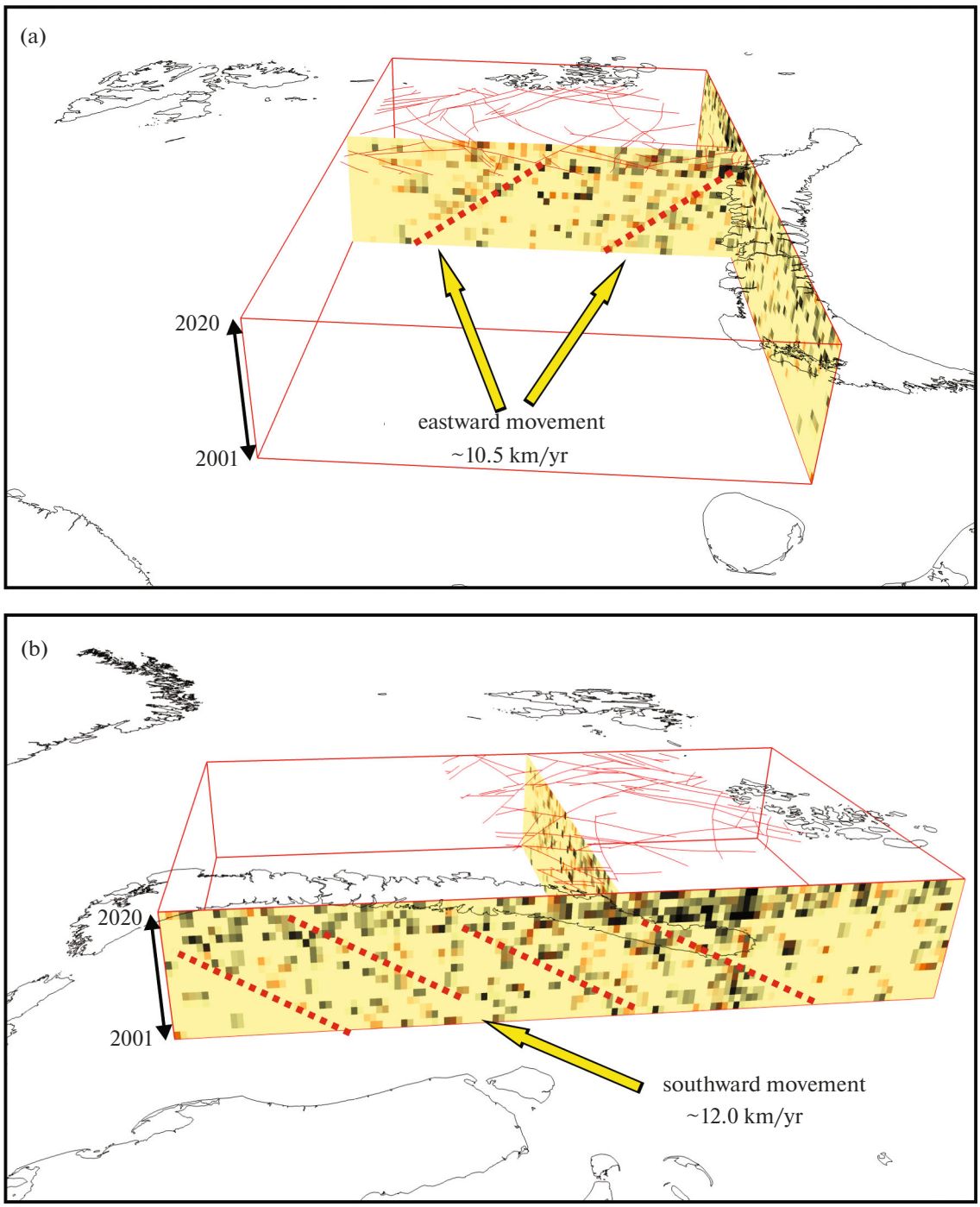

Fig. 5. Total seismic moment (between 0 and 155 × 10^{13} J) in the eastern Barents Sea in (10 × 10 km) × (1 year) grid meshes based on NORSAR data (*NORSAR* ..., 2022) for the period 2001–2020. We used events with magnitudes upward of –2. The 1 : 1 000 000 fault network is based on Sheet T-37-40 (*Karta* ..., 2004]). Arrows indicate trends of space–time movement of energy release at apparent velocities along the vertical slices through the three-dimensional array. (a) View from the south to north, an east–west cross section of total seismic moment, (b) view from east to west, a north–south cross section of total seismic moment.

them, but the available data enable us to find some quantitative characteristics and likely cause-and-effect relations among them. As well, we might try to compare the rates of space–time migration of seismic activity due to the tectonic deformation waves within the shelf toward the AARS segments.

The rate of tectonic deformation waves accompanied by seismic tremor can reach 10–15 km/year at

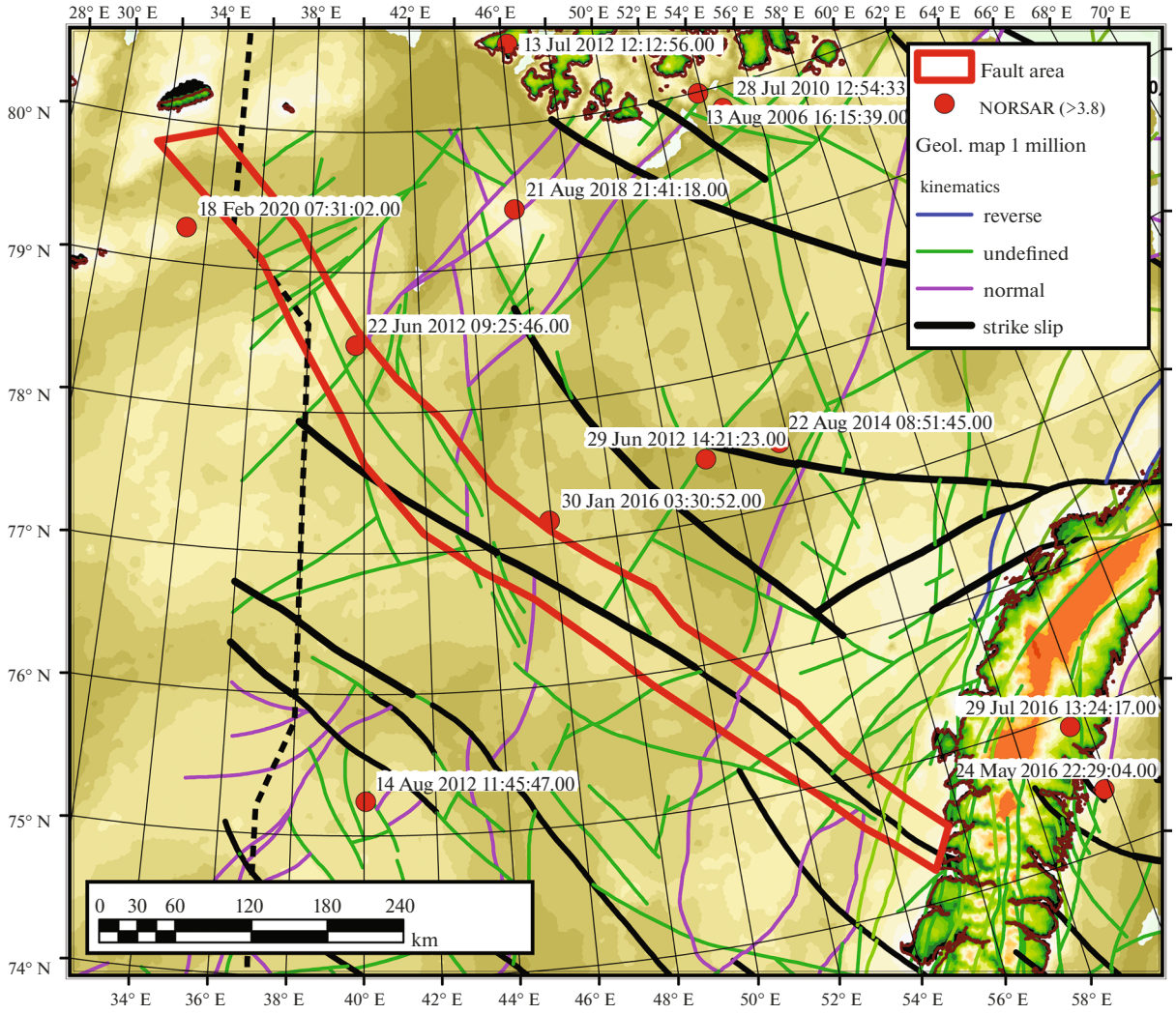

Fig. 6. The area of seismicity analysis based on data of (*NORSAR* ..., 2022) along the zone of a linear epicenter clustering (see Fig. 2) on the fault network as depicted in the State Geological Map of the Russian Federation, scale 1 : 1000000 (the New Series) with the faults indication by kinematic type of movement after (*Karta* ..., 2004). The epicenters are shown for magnitudes greater than >3.8.

short fault segments (Bykov, 2005, 2018), and can increase attaining a few hundred kilometers per year on long tectonic features like subduction zones. The basis for the determination of rates is a space–time representation of the seismic process which, when within the fault zone of the shelf (see Figs. 5a, 5b), gives ~10.5 and ~12.0 km/year when projected onto the X and Y axes, respectively, while the values along the fault are ~22.8 and ~25.7 km/year (see Fig. 7). One notes a higher release of seismic energy in 2012 and during the time between 2016 and 2020. We have calculated total moments from yearly values for the shelf fault zone from data of (*NORSAR* ..., 2022), and compared these with the total moments for the Knipovich and Gakkel ridges based on data from (*USGS* ..., 2022) and for the area of intrashelf seismicity off the Spitsbergen Archipelago from data of (*ISC* ..., 2023) (without the Novaya Zemlya data) (Fig. 9) using the procedure for comparing minima displaced over time as described by Antonovskaya et al. (2021), with the only modification that minima have been replaced with maxima.

The plots show both yearly sums and averaged values in a moving window of 3 years. One can see the evolution of moment release in a smoother form. It would have been unreasonable to use a longer window, 5 years of still more, because that would produce spurious minima in those time intervals where local maxima of the moment occur in the original data. One of the chief features noticeable in the plotted moments for the nearly orthogonal AARS segments consists in synchronicity in the occurrence of maxima (see Fig. 9). The shaded bands mark the segments of synchronous peaks for the Knipovich and Gakkel ridges. One especially notes the silent interval during the period from 1968 to 1988, identical in both plots. This character of

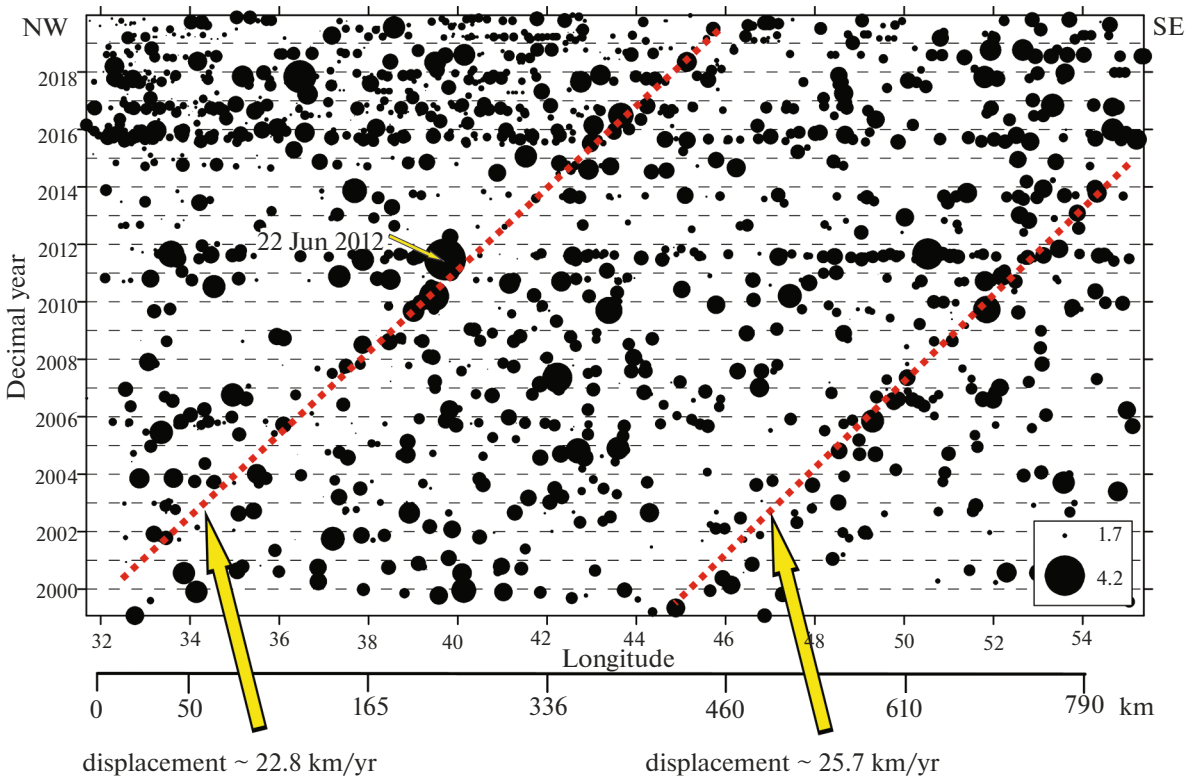

Fig. 7. The space-time structure of seismicity based on data of (*NORSAR* ..., 2022) along the area of analysis (see Fig. 6) in a band near the fault having a linear clustering of epicenters. The horizontal longitude scale is supplemented with the distance along the area in kilometers. Arrows and numerals indicate the trend lines and the rates of energy release movement along them.

seismic energy release indicates the presence of a planetary factor serving as a trigger for the release of tectonic stresses (or for magma ascent) in the AARS segments located ~1000 km apart without a time lag.

Figure 9 shows the total moment for the fault zone (see Fig. 6) along which trends of activity migration have been identified (see Figs. 5a, 7). One feature of total moment behavior is a 12-year "silent" interval until the 2012 peak, which has no analogue in the AARS (see Figs. 9a, 9b). The 2016–2020 maximum has an analogue in the AARS maxima and in the shelf as can be seen from the data of (*ISC* ..., 2023) (see Fig. 9d). This may also be an indication of a common trigger for all areas during the studied time period. Supposing that the plot of total moment for the fault zone was due to a delayed triggering from the AARS segments, then it would be reasonable to compare it with peaks preceded by long enough silent periods. Assuming that the peaks are those of 1963 and 1966 occurring at the Gakkel and Knipovich ridges, respectively, we get the rates ~20.8 and ~22.0 km/year, which are in good agreement with the rate of migration in the fault zone determinable from data at many sites (see Figs. 5a, 7). If we compare the plot of Fig. 9c with those of 1991 and 1998, we get the rates ~50 and ~77 km/year, which are reasonable values as well. Garagash and Lobkovsky (2021) and Lobkovsky et al. (2023) determined the rate at which tectonic deformation waves travel, namely, ~100 km/year for the Arctic and Antarctica. The waves were generated by great events at subduction zones. No such waves occur along the framing of the Barents Sea, but in consideration of a planetary character of these events and the associated deformation waves, one may well hypothesize that they also exerted some impact on the AARS as well, and on the shelf area.

Our calculations of the moments shown in Fig. 9b did not incorporate the intraplate seismicity south of the Spitsbergen Archipelago, as being irrelevant to the AARS rift structure. The data for this region were obtained from the catalog in (*ISC* ...., 2023), with the calculated values for individual years being shown in Fig. 9d. Unfortunately, this catalog does not contain large events for the area of the northwest striking fault for which we have used the (*NORSAR* ..., 2022) catalog. Applying the above approach to the 2012 peak in Fig. 9c for comparison with the 1976 and 2003 maxima in the ISC catalog with silent periods before them (see Fig. 9d), we get rates of hypothetical displacement as ~17 and ~67 km/year, respectively, which provide a range similar to the values based on the AARS maxima (see Figs. 9a, 9b).

Supposing that the propagation of a deformation wave from the AARS that triggers local seismicity on

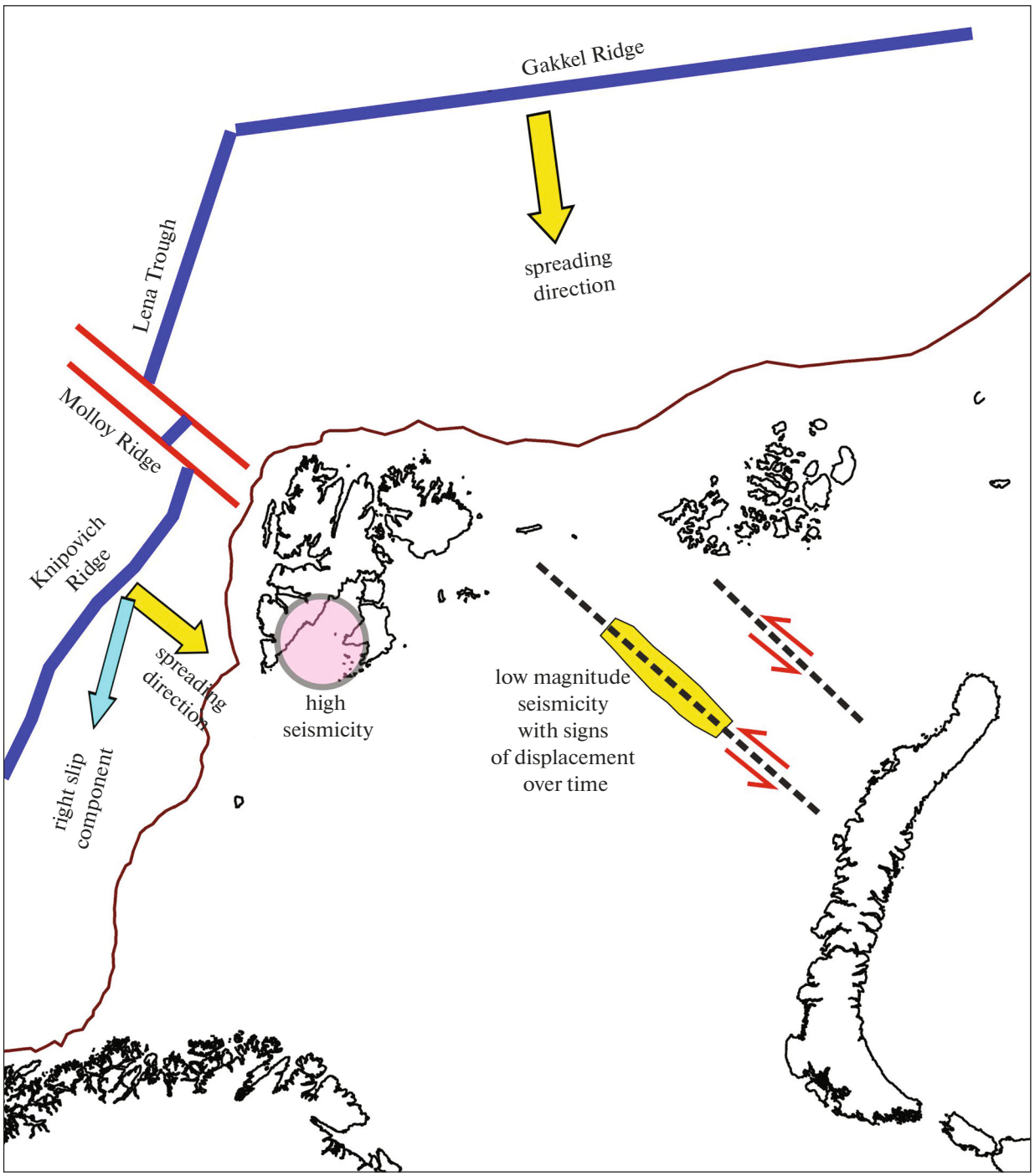

Fig. 8. A map showing the geodynamics of the study area with elements that are required for interpretation of tectonics within the Barents Sea shelf. The dimensions of the vectors representing the action on the plate are conventional.

the fault and, traversing the intraplate area where large events occur, influences that area as well, then we infer that the rates of propagation from the AARS to the zone located to the south of the Spitsbergen Archipelago must also be comparable with those which we have determined by comparison with the fault zone. The 1976 and 2003 peaks do not fit the general pattern of synchronous energy release along the AARS, even though the areas are close to one another geographically. From this we might infer a possible influence of the AARS on the seismic process in the western part of the shelf. We estimated the rates for these peaks based on displacements of similar peaks along the AARS as ~44 and ~36 km/year, respectively (see Fig. 9d).

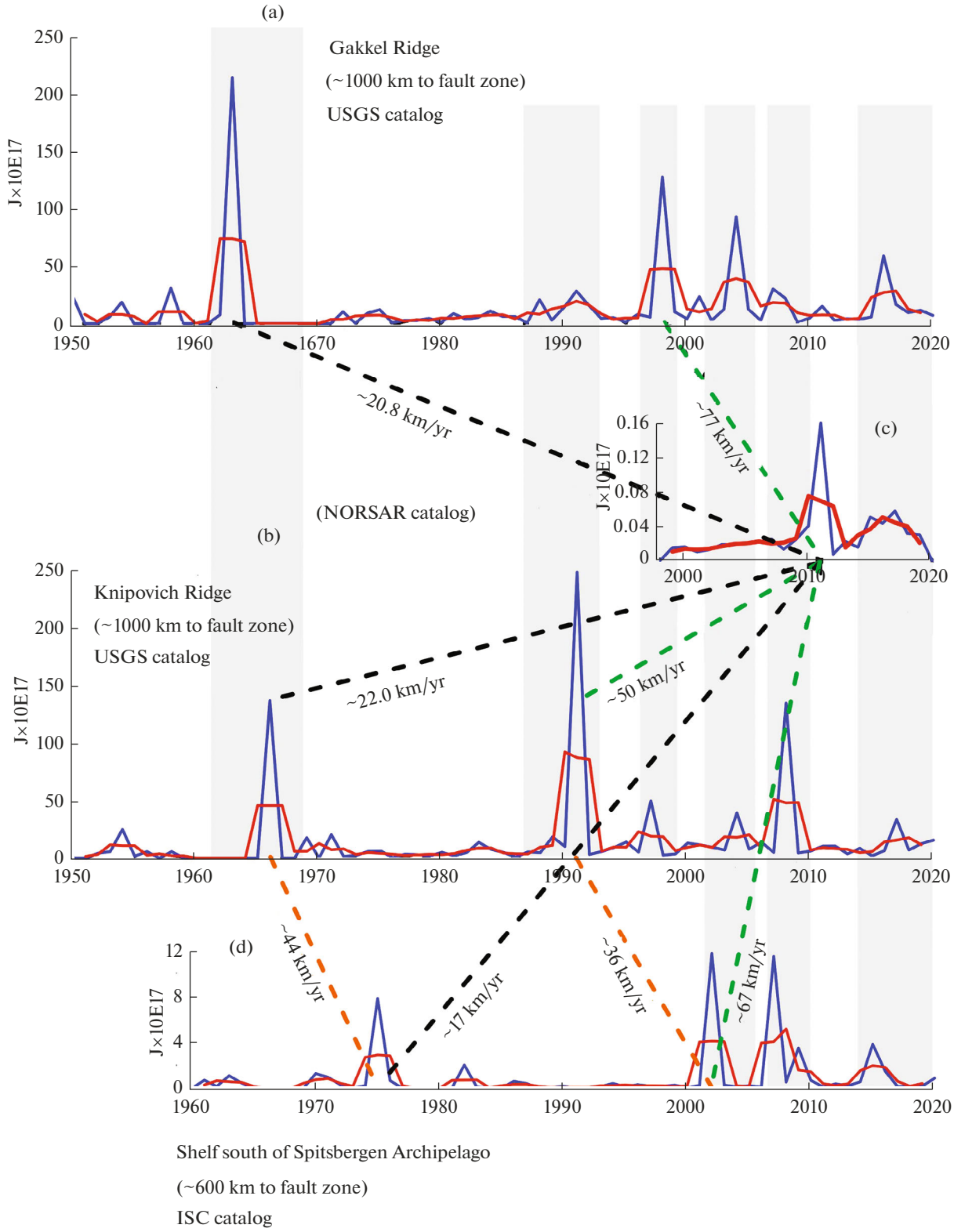

Fig. 9. The temporal structure of total seismic moment for ridges Gakkel (a) and Knipovich (b) based on data of (*USGS* ..., 2022), along the area of analysis (see Fig. 6) in a band near the fault with linear clustering of epicenters (c) based on data of (*NORSAR* ..., 2022), and in the shelf area south of the Spitsbergen Archipelago (d) based on data of (*ISC* ..., 2023). Dark blue lines show plots of total seismic moment over individual years. Red lines are plots as smoothed in a moving window of 3 years. The distances from the ridges and intraplate seismicity are measured to the middle of the fault zone perpendicularly to the spreading axes. The numerals at the inclined lines give estimated rates of movement for moment extremums in space. Grey shaded areas show some zones of synchronous extremums with different amplitudes.

A likely explanation of these values might consist in the fact that the deformation wave travels over the oceanic part of the total path at rates that are twice as high as those for the shelf part.

We think that, considering the case of the Barents Sea, we should prefer the solution giving rates close to the values 10–22 km/year, since the latter are approved for short fault segments with continuous tracing from year to year on a 10-km spatial grid, as, e.g., in Fig. 5a or Fig. 7. Comparison between peaks at structures that are far from each other may be wrong, because no continuous tracing occurs between them. In seismic prospecting, satisfactory correlation between reflectors is achieved for the case in which the Fresnel zone coverage is at least 50%. In a similar manner, when dealing with seismically active structures, the possible progress of a deformation wave can be reliably determined using a sequence of objects that are more closely packed, because one can make mistakes in comparisons of moment maxima at a distance of 1000 km. We believe that in the case where there is direct push of a ridge structure on the sides of a strike slip fault or a trigger initiation by a large event, the seismic moment peaks in the AARS and in the shelf must be synchronous without time shifts. Such a coincidence is only observed for the period from 2016 to 2020.

CONCLUSIONS

1. Weak seismic events as recorded by the NORSAR regional network within the Russian part of the Barents Sea shelf for the period from 2001 to 2020 align to form linear clusters along strike slip faults that have been reliably identified by structural 2D seismic prospecting. The faults are oriented at an angle of ~45° with respect to the geodynamically active segments of the Atlantic–Arctic Rift System, namely, the Knipovich and Gakkel ridges that make a framing of the shelf to the west and north.

2. The fault network that has been determined by structural seismic prospecting and high frequency profiling displaces Mesozoic seismic sequences and emerges at the bottom surface, displacing Quaternary deposits, and clearly indicating a present-day age for the dislocations to which the linear clusters of weak seismicity are confined.

3. Calculation of the total seismic moment in the space–time dimension showed the presence of an east–west seismicity migration eastward along short fault segments in the shelf at a rate of 10.5 km/year, with a concurrent north–south migration southward at a rate of 12.0 km/year. The migration of seismic activity along the fault zone to which the best-pronounced linear cluster of weak events is confined occurs at a rate of 22.8 to 25.7 km/year. One notes a burst of general activity in the shelf area beginning in 2012.

4. Comparison of the time-dependent evolution of seismic activity in the shelf with similar plots for fragments of the AARS, and of the active zone within the shelf, suggests that it was caused by tectonic deformation waves initiated along a geodynamically active interplate boundary and traveling within the shelf at a rate of 20–22 km/year. A less likely scenario consists in the excitation due to the rift system that travels at rates of between 50 and 77 km/year, because the areas being compared are far from each other, while the rate between 22.8 and 25.7 km/year within the shelf fault zone is reliably identified from continuous displacements of the moment values at short spatial segments.

5. The increase in seismicity intensity in the shelf after 2012 does not seem to have been emission due to the excitation of a slow deformation wave traversing a structural inhomogeneity identified by seismic prospecting. This maximum of the moment in the fault zone in the shelf is synchronized with analogous maxima in the AARS rift structures and in the shelf south of the Spitsbergen Archipelago, thus indicating a possible direct triggering excitation by AARS structures.

ACKNOWLEDGMENTS

We are grateful to the crew of the R/V *Akademik Boris Petrov* and to the research team of the 51st cruise (October–November 2022) for their commitment under severe conditions in acquiring the field materials used in the present study. We also thank the Russian Federal Geological Foundation (https://rfgf.ru) for access to seismic data acquired for the northern Barents Sea.

FUNDING

This work was supported by the Russian Science Foundation through project no. 22-27-00578 "Recent and modern geodynamics of the Western Arctic: evolution and impact of active tectonic processes on structural elements and sedimentary cover of deep-sea basins and shelves."

CONFLICT OF INTEREST

The authors of this work declare that they have no conflicts of interest.

REFERENCES

Antonovskaya, G.N., Basakina, I.M., Vaganova, N.V., et al., Spatiotemporal relationship between Arctic mid-ocean ridge system and intraplate seismicity of the European Arctic, *Seismol. Res. Lett.,* 2021, vol. 92, pp. 2876–2890. https://doi.org/10.1785/0220210024

Boldyrev, S.A., *Seismogeodinamika Sredinno-Atlanticheskogo khrebta* (The Seismic Geodynamics of the Mid-Atlantic Ridge), Moscow: NGK RF, 1998.

Bungum, H., Ritzmann, O., Maercklin, N., et al., Three-dimensional model for the crust and upper mantle in

the Barents Sea region, *Eos,* 2005, vol. 86, no. 16, pp. 1–3.

Bykov, V.G., Strain waves in the Earth: The concept, observations, and models, *Geol. Geofiz.*, 2005, vol. 46, no. 11, pp. 1176–1190.

Bykov, V.G., Prediction and observation of strain waves on Earth, *Geodyin. Tekton.*, 2018, vol. 9, no. 3, pp. 721–754. https://doi.org/10.5800/GT-2018-9-3-0369

Crane, K., Doss, S., Vogt, P., Sundvor, E., Cherkashov, I.P., and Devorah, J., The role of the Spitsbergen shear zone in determining morphology, sedimentation and evolution of the Knipovich Ridge, *Marine Geophys. Res.,* 2001, vol. 22, pp. 153–205.

Dunaev, N.N., Levchenko, O.V., Merklin, L.R., and Pavlidis, Yu.A., The Novaya Zemlya shelf during Late Quaternary time, *Okeanol.,* 1995, vol. 35, no. 3, pp. 440–450.

Gac, S., Klitzke, P. Minakov, A., Faleide, J.I., and Scheck-Wenderoth, M., Lithospheric strength and elastic thickness of the Barents Sea and Kara Sea region, *Tectonophysics,* 2016, vol. 619. https://doi.org/10.1016/j.tecto.2016.04.028

Garagash, I.A. and Lobkovsky, L.I., Tectonic strain waves as a possible triggering mechanism to activate the emission of methane in the Arctic, Arktika: Ekologiya i Ekonomika, 2021, vol. 11, no. 1, pp. 42–50. https://doi.org/10.25283/2223-4594-2021-1-42-50

GPS Time Series Data, 2022, Jet Propulsion Laboratory of California Institute of Technology. https://sideshow.jpl.nasa.gov/post/series.html.

Gusev, E.A. and Shkarubo, S.I., The anomalous structure of the Knipovich Ridge, *Ross. Zhurn. Nauk Zemle,* 2001, vol. 3, no. 2, pp. 165–182.

Harrison, J.C., St-Onge, M.R., Petrov, O.V., et al., *Geological Map of the Arctic 1 : 5000000,* Geological Survey of Canada, 2008, Open file report 5816.

Heflin, M., Donnellan, A., Parker, J., Lyzenga, G., Moore, A., Ludwig, L.G., Rundle, J., Wang, J., and Pierce, M., Automated estimation and tools to extract positions, velocities, breaks, and seasonal terms from daily GNSS measurements: Illuminating nonlinear Salton Trough deformation, *Earth and Space Science,* 2020, vol. 7, no. 7. e2019EA000644. https://doi.org/10.1029/2019EA000644

ISC Bulletin: Event Catalogue Search, 2023 (Sampled July 11, 2023). http://www.isc.ac.uk/iscbulletin/search/catalogue/ https://doi.org/10.31905/D808B830

Jakobsson, M., Mayer, L.A., Bringensparr, C., et al., The International Bathymetric Chart of the Arctic Ocean version 4.0, Nature. *Scientific Data*, 2020, vol. 7, no. 176. https://doi.org/10.1038/s41597-020-0520-9

Karta dochetvertichnykh obrazovanii (A Map of Pre-Quaternary Rocks). T-37-40 (Franz Josef Land, Southern islands). The state geological map of the Russian Federation to scale 1 : 1 000 000 (New Series). Sheet 1, Lopatin, B.G., Editor-in-Chief, St. Petersburg: MAGE, PMGRE, VNIIOkeanologiya, 2004.

Keiding, M., Olesen, O., and Dehls, J., *Neotectonic Map of Norway and Adjacent Areas, Scale 1 : 3000000,* Geological Survey of Norway, 2018.

Khain, V.E. and Lomize, M.G., *Geotektonika s osnovami geodinamiki* (Geotectonics with Principles of Geodynamics), Moscow: KDU, 1995.

Khutorskoi, M.D., Leonov, Yu.G., Ermakov, A.V., and Akhmedzyanov, V.R., Anomalous heat flow and the origin of trenches in the northern Svalbard plate, *Dokl. Akad. Nauk,* 2009, vol. 424, no. 2, pp. 318–323.

Krapivner, R.B., Signs of neotectonic activity in the Barents Sea shelf, *Geotekt.,* 2007, no. 2, pp. 73–89.

Krapivner, R.B., *Krizis lednikovoi teorii: argumenty i fakty* (A Crisis in Glacial Theory: Arguments and Facts), Moscow: GEOS, 2018.

Kutinov, Yu.G., Chistova, Z.B., and Belenovich, T.Ya., The Arctic marginal planetary zone, *Arkt. Ekol. Ekon.,* 2015, no. 4 (20), pp. 38-47.

Lobkovsky, L.I., Baranov, A.A., Ramazanov, M.M., Vladimirova, I.S., Gabsatarov, Yu.V., and Alekseev, D.A., A possible seismogenic triggering mechanism for methane emission, erosion of glaciers, and climate warming in the Arctic and Antarctica, *Fizika Zemli,* 2023, no. 3, pp. 33–47. https://doi.org/10.31857/S0002333723030080

Morozov, A.N., Vaganova, N.V., and Konechnaya, Ya.V., The seismicity of the northern Barents Sea in the area of the Franz–Victoria and Orly troughs, *Geotekt.,* 2014, no. 3, pp. 78–84.

Morozov A.N., Vaganova N. V., Konechnaya Y.V., Asming V.E. New data about seismicity and crustal velocity structure of the "continent–ocean" transition zone of the Barents-Kara region in the Arctic, *J. Seismol.,* 2015, vol. 19, pp. 219–230.

Musatov, E.E., The structure of the Cenozoic cover and the neotectonics of the Barents-Kara shelf as inferred from seismoacoustic observations, *Ross. Zhurn. Nauk Zemle,* 1998, vol. 1, no. 2, pp. 157–183.

Nikitin, D.S., Gorskikh, P.P., Khutorskoi, M.D., and Ivanov, D.A., Structural and tectonic features of the northeastern Barents Sea plate based on data of numerical modeling of potential fields, *Geotekt.,* 2018, no. 2, pp. 58–75. https://doi.org/10.7868/S0016853X18020042

NORSAR Seismic Bulletins, 2022 (Sampled March 1, 2022). https://doi.org/10.21348/b.0001 https://www.norsar.no/seismic-bulletins/.

Olesen, O., Riis, F., Lindholm, C.D., Dehls, J.F., Hicks, E.C., and Bungum, H., *Neotectonic Map, Norway and Adjacent Areas, Scale 1 : 3000000,* Geological Survey of Norway, 2000.

Ritzmann, O., Maercklin, N., Faleide, J.I., Bungum, H., Mooney, W.D., and Detweiler, S.T., A 3D geophysical model for the crust in the greater Barents Sea region: Database compilation, model construction and basement characterization, *Geophys. J. Int.,* 2007, vol. 170, pp. 417–435. https://doi.org/10.1111/j.1365-246X.2007.03337.x

Shipilov, E.V., On the tectono-geodynamic evolution of the Arctic continental margins during young ocean generation epochs, *Geotekt.,* 2004, no. 5, pp. 26–52.

Shipilov, E.V., Late Mesozoic magmatism and Cenozoic tectonic deformations in the Barents Sea continental margin: The influence on the distribution of hydrocarbon potential, *Geotekt.,* 2015, no. 1, pp. 60–85.

Shipilov, E.V. and Shkarubo, S.I., *Sovremennye problemy geologii itektoniki osadochnykh basseinov Evroaziatsko-Arkticheskoi kontinentalnoi okrainy* (Modern Problems in the Geology and Tectonics of Sedimentary Basins of the Eurosian-Arctic Continental Margin), vol. 1 (*Litologo-stratigraficheskie kompleksy osadochnykh basseinov Barentsevo-Karskogo shelfa*) (Lithologic and Stratigraphic Complexes of Sedimentary Basins in the Barents-Kara Shelf), Apatity: KNTs RAN, 2010.

Sirotkin, A.N. and Sharin, V.V., The age of Quaternary volcanic occurrences in the Bjkfjorden area in Spitsbergen Archipelago, *Geomorfol.,* 2000, no. 1, pp. 95–106.

Sokolov, S.Yu., Abramova, A.S., Moroz, E.A., and Zaraiskaya, Yu.A., The amplitudes of discontinuities at the flanks of the Knipovich Ridge, North Atlantic Ocean, as an indicator of present-day geodynamics of the region, *Geodin. Tekton.,* 2017, vol. 8, no. 4. C. 769–789. https://doi.org/10.5800/GT-2017-8-4-0316

Sokolov, S.Yu., Abramova, A.S., and Shkarubo, S.I., Neotectonic discontinuities in the Barents Sea and their genesis based on data from bottom morphometry, seismic prospecting, and deep mantle structure, *Dokl. Akad. Nauk, Nauki o Zemle,* 2023a, vol. 509, no. 1, pp. 62–68. https://doi.org/10.31857/S2686739722602484

Sokolov, S.Yu., Agranov, G.D., Shkarubo, S.I., and Grokholsky, A.L., The southeastern flank of the Knipovich Ridge, North Atlantic: Basement structure and neotectonics based on geophysical data and experimental modeling, *Geotekt.,* 2023b, no. 1, pp. 1–18. https://doi.org/10.31857/S0016853X2301006X

Solheim, A., Musatov, E., and Heintz, N., *Geological Aspects of Franz Josef Land and the Northernmost Barents Sea, Meddelelser,* 1998, no. 151, Oslo: Norsk Polarinstitutt.

USGS Search Earthquake Catalog, 2022 (Sampled January 17, 2022). earthquake.usgs.gov/earthquakes/search/.

Verba, V.I., Avetisov, G.P., and Stepanova, T.V., Geodynamics and magnetism in the basalts of the Knipovich undersea ridge, Norwegian–Greenland basin, *Ross. Zhurnal Nauk o Zemle,* 2000, vol. 2, no. 4, pp. 3–13.

Vinogradov, A.N., Verba, M.L., Verba, V.V., et al., An outline of the geological structure of the Euro-Arctic region, in *Stroenie litosfery rossiiskoi chasti Barents-regiona* (The Lithosphere Structure of the Russian Part of the Barents Region), Sharov, N.V., Mitrofanov, F.P., Verba, M.L., and Gillen, K., Eds., Petrozavodsk: Karelsky NTsRAN, 2005, pp. 16–39.

Yakovlev, A.V., Bushenkova, N.A., Kulakov, I.Yu., and Dobretsov, N.L., The structure of upper mantle in the Arctic region as determined using regional seismic tomography, *Geol. Geofiz.,* 2012, vol. 53, no. 10, pp. 1261–1272.

Zaraiskaya, Yu.A., Segmentation and seismicity of ultraslow mid-oceanic ridges: The Knipovich and Gakkel ridges, *Geotekt.,* 2017, no. 2, pp. 67–80.

Zykov, D.S. and Baluev, A.S., The character and causes of neotectonic deformations in the northwestern Barents Sea plate, Svalbard Archipelago, *Byull. MOIP, Otdel Geol.,* 2008, vol. 83, no. 6, pp. 20–26.

Translated by A. Petrosyan